A NOVEL HYBRID SOLAR POWER GENERATION SYSTEM USING A-SI PHOTOVOLTAIC/THERMAL COLLECTORS AND ORGANIC RANKINE CYCLE

Jing Li, Pengcheng Li, Gang Pei*, Jie Ji, Jahan Zeb Alvi, Lijun Xia

Department of Thermal Science and Energy Engineering, University of Science and Technology of China,
Hefei, Anhui, China
E-mail: peigang@ustc.edu.cn; lijing83@ustc.edu.cn

ABSTRACT

A novel hybrid solar power generation system (HSPGS) is proposed. It mainly consists of photovoltaic/thermal (PV/T) collectors based on amorphous silicon (a-Si) cells, organic Rankine cycle (ORC), and inner-type heat storage unit. The PV/T collectors produce electricity directly via the cells, and the waste heat is carried away to the ORC for thermal power generation. Owing to the unique effect of thermal annealing, a-Si cells together with the ORC benefit from high temperature operation. Steady power generation is guaranteed by the heat storage unit. Compared with the conventional PV and solar ORC systems, the HSPGS can avoid or greatly reduce the usage of expensive battery, and has a much higher power efficiency. This work presents a close view of the HSPGS. Mathematic models are built and the system performance in the temperature range from 80°C to 150°C is estimated. Efficiency of about 12.5% can be achieved with a hot side temperature of 100°C.

1. INTRODUCTION

Solar ORC from tens of kWe to a few hundred kWe has great potential to meet the residential demand on heat and power. It has advantages over the highly concentrated solar thermal power technology in regard to the easier energy collection and storage, and the ability to supply energy near the point of usage. However, one critical problem of solar ORC is the low power efficiency. With a hot side temperature of 150 °C, the power efficiency is expected to be lower than 7%.

Photovoltaic (PV), is a simpler and more efficient way to generate electricity from solar irradiation. Heat can be also supplied to the consumers via the PV/T technology. Both power efficiency and cost-effectiveness of PV cells have been improved significantly in the past 10 years. One of the challenges associated with solar PV system is the energy storage. Currently lots of the PV systems are connected to the electric grid. Solar cells will generate electricity steadily throughout the day as long as the sun is shining. But when the sky is partly cloudy, solar power output from an entire region can fluctuate unpredictably. To mitigate the impact of this phenomenon, energy storage is a vital component of a more resilient, reliable and efficient electric grid. Energy storage will help lower consumer costs by saving low-cost power for peak times and making renewable energy available when it's needed the most. Aside from the grid-tied system, the off-grid PV system is preferable in remote areas for the sake of a silent, emission-free energy source, avoidance of the high cost of extending a utility line, and independence of homemade energy production. A backup energy source is essential for the stand-alone PV system. Unfortunately, the deployment of battery storage will dramatically increase the system cost. With a 5h lithium battery storage, the total system cost will be 30500RMB (about 5000 US$)/kW, which is 4 times of that without storage (Li *et al.,* 2015).

Solar ORC technology is frequently compared with the PV technology to clarify its advantages. Nevertheless, cooperation of the two technologies can be more beneficial. A hybrid solar power generation system (HSPGS) based PV/T and ORC technologies is described in a patent (Li *et al.,* 2009). The cells absorb solar energy, part of which is converted into electricity directly and the rest is converted into heat. The heat is further utilized to drive the ORC and generate electricity. The HSPGS has the advantages over the conventional PV system regarding the replacement of expensive battery storage by heat storage, and is much more efficient than the solo solar ORC. Research on the HSPGS has also been reported (Li *et al.,* 2010, Kosmadakis *et al.,* 2011).

The selection of PV material is crucial for the HSPGS. Crystalline silicon (c-Si) cell has a high temperature coefficient of power at maximum power point (PMPP), which is about -0.41 to -0.50%/°C at standard test conditions (STC). The coefficient is negative with larger magnitude at higher temperature (King *et al.,* 1997). Given an efficiency of 18% at 25°C, the absolute decrement in the efficiency can be more than 10% when the operating temperature increases to 150°C. Gallium arsenide (GaAs) cell has a relatively low temperature coefficient of PMPP of about -0.20%/ °C, but its efficiency at 25°C is generally higher than 25%, which may drop to 18% at 150°C. In the case of the c-Si and GaAs solar cells, the efficiency superiority of the HSPGS is not significant due to the great efficiency loss of the cells at high temperature. Though amorphous silicon (a-Si) cell is less efficient than c-Si and GaAs cells at normal operating temperature, it seems more suitable for the HSPGS application.

2. CHARATERISTICS OF A-SI CELL

a-Si is the non-crystalline allotropic form of silicon. a-Si cell is the most well developed thin film cell. In China a total capacity more than 2.0 GW of a-Si cell can be produced annually (Hanergy, 2015). It can be deposited at low temperature onto a variety of substrates such as glass, plastic and metal, and thus produces savings on silicon material cost. One compelling characteristic of a-Si cell is the degradation in the power output when exposed to the sunlight, which is known as the Staebler–Wronski Effect (SWE). It is easy to achieve an initial a-Si cell efficiency of 10%, but it will drop to 7% or lower at stabilized state. The SWE has limited the development of a-Si cell despite of its relatively low cost, and makes it less competitive with c-Si cell. Notably, the common use of a-Si cell is subject to the ambient temperature. At higher operating temperature (>50°C), a-Si cell will benefit from the thermal annealing (Fanni *et al.,* 2009). The defects induced by light will decrease and even disappear, leading to an improved power generation.

A number of experiment results have indicated that a-Si cells perform better at higher operating temperature. For example, Del Cueto *et al.*(1999) investigated the temperature–induced changes in the performance of a-Si modules from different manufacturers in controlled lighit-soaking. Exposure of the modules was executed at low temperature (22±8°C) for about 1000 h, which was subsequently followed up with exposure at warm temperature (51±8°C) for about 500 h. The degradation at low temperature was recovered upon the subsequent warm soaking, resulting in an efficiency increment between 10% and 17%. Further investigation showed the operating temperature during light-soaking was the most important factor for determining stabilized cell performance, while the light intensity seemed to be the least important one (Roedern *et al.,* 2000). According to the four-year experiment conducted later on, higher minimum operating temperature leaded to higher performance levels of a-Si cell (Ruther *et al.,* 2005). Nikolaeva - Dimitrova *et al.* (2010) compared the seasonal variations on energy yield of a-Si, hybrid, and c-Si PV modules. The average efficiency of thin film modules in the hot month was greater than that in the cold month. Makrides *et al.* (2012) analyzed the effect of temperature on different grid-connected PV technologies over the period June 2006-June 2010. An increase in power for all the a-Si technologies was obvious during the warm summer season. These oscillations were due to both spectral effect and SWE. With the same spectral distribution, the efficiency of a-Si cell at mid-August was 8% higher than that at mid-February (Virtuani *et al.,* 2014). The dynamic degradation of a-Si cell at 25, 50 and 90°C was monitored (Pathak *et al.,* 2012a, Pathak *et al.,* 2012b, Rozario *et al.,* 2014). Higher operating temperature resulted in faster degradation and higher efficiency at degraded steady state (DSS). Some of the results are presented in Figure 1.

As demonstrated in the above works, the temperature coefficient of PMPP of a-Si cell at DSS is positive, which is contrary to that at STC. A value of about -0.21%/°C is common at STC. However, duration of the test is typically short. The cell is unable to experience a full annealing or degradation as the operation temperature changes. Evidences have shown the temperature coefficient of PMPP of a-Si cell for a short time scale of several hours is negative, while it is positive for a longer time scale of seasons (Ishii *et al.,* 2011). In fact, a-Si modules continue to show further change in maximum power even after they stabilize according to the international qualification standard IEC 61646. To perform sufficient preconditioning of thin-film modules prior to precision calibration, a new more complete standard procedure is needed (Kenny *et al.,* 2014).

The unique effect of thermal annealing makes a-Si cell especially suitable for PV/T application, where

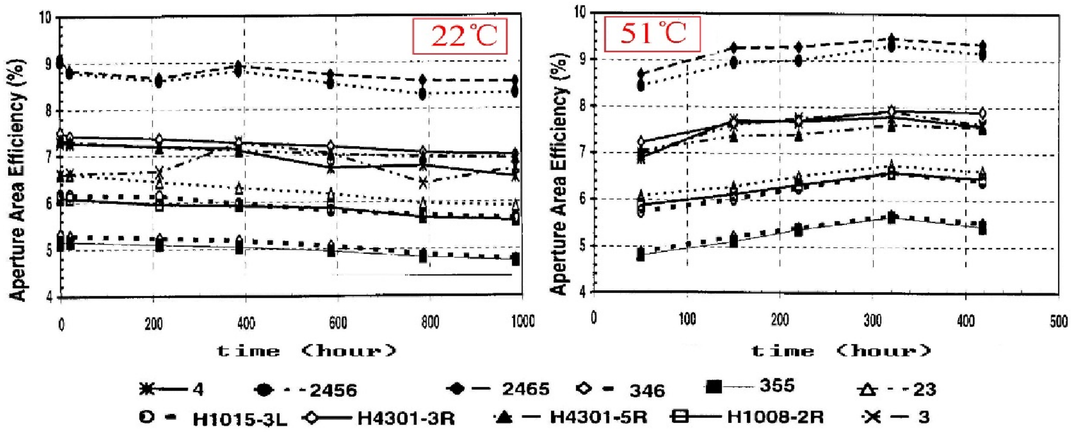

(a)

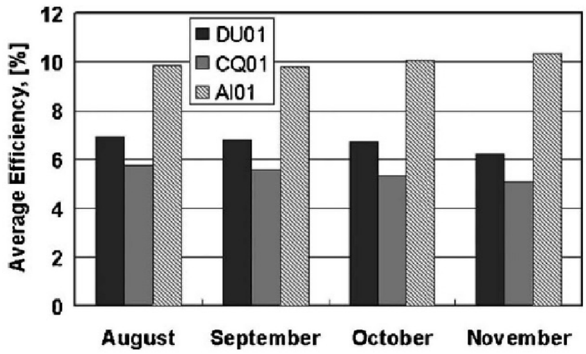

(b) DU:a-Si/μ-Si, CQ: a-Si, Al: c-Si,

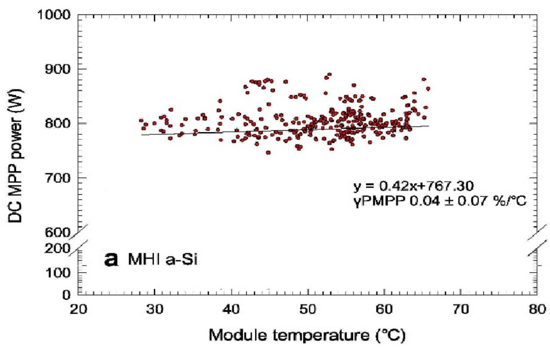

(c)

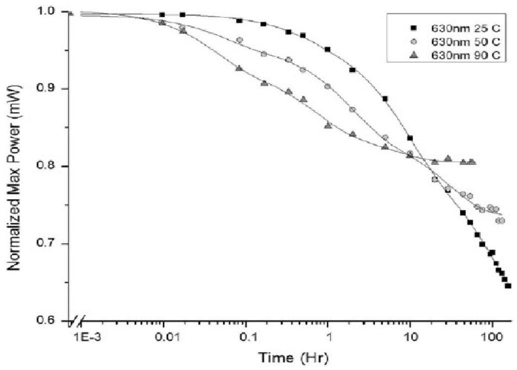

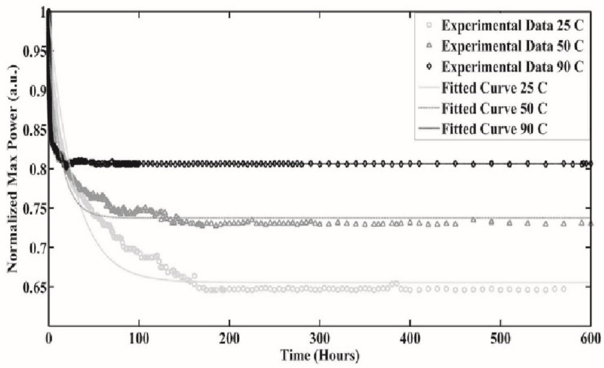

(d)

Figure 1: Variations of a-Si cell efficiency and power with time and operating temperature (a) by Del Cueto et al.,(b) by Nikolaeva -Dimitrova et al.,(c) by Makrides et al., (d) by Pathak et al.

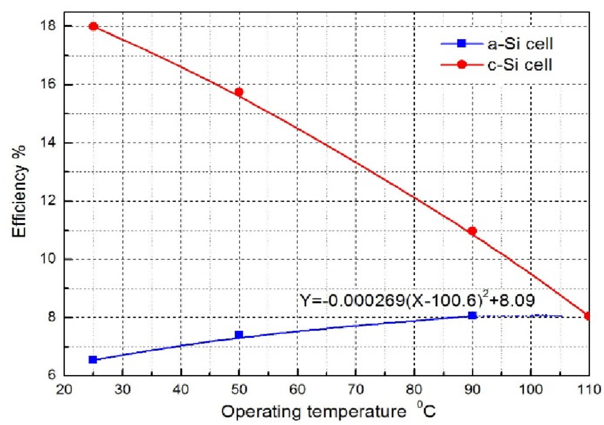

Figure 2: Variations of a-Si and c-Si cell efficiencies with the operation temperature

the operation temperature is higher than the ambient temperature. Research on the a-Si PV/T system is accumulating (Nualboonrueng *et al.,* 2012, Rahou *et al.,* 2014, Gaur *et al.,* 2014, Rozario *et al.,* 2014, Aste *et al.,* 2015). A comparison between a-Si and c-Si cell efficiencies at DSS under different operation temperature is shown in Figure 2 by using the results in Figure 1(d). At higher temperature, a-Si cell is competitive with c-Si cell in view of the efficiency, and the former is cheaper.

3. SYSTEM DESTRIPTION

The proposed HSPGS is shown in Figure 3. The system is composed of PV/T collectors, pumps, fluid storage tank with phase change material (PCM), expander, generator and condenser. It has the following innovative features:

(1) a-Si cells characterized by positive temperature coefficient of PMPP at DSS are employed.
(2) The working fluid is vaporized directly in the PV/T collectors.
(3) An inner-type heat storage unit is embedded in the ORC to guarantee the stability of power generation.
(4) The system is the first of its kind.

There are many types of collectors suitable for the medium-high temperature PV/T application, such as compound parabolic concentrators (CPC), evacuated tube heat pipe collectors, and evacuated flat plate collectors (FPC), as schematized in Figure 4. CPC collectors with small concentration ratio are able to accept a large proportion of the diffuse radiation incident on their apertures and concentrate it without the need of tracking the sun. CPCs would substantially performance better than FPCs at temperature above 80 ºC while requiring only several adjustments for year-round operation. The evacuated tube heat pipe collectors use liquid–vapor phase change materials to transfer heat at high efficiency. These collectors feature a heat pipe (an excellent thermal conductor) placed inside a vacuum-sealed tube. The pipe is made of copper and attached to a black or blue fin that fills the tube. Both the pipe and fin absorb solar radiation. The fluid inside the pipe undergoes an evaporating-condensing cycle. The commercial collectors of this type are able to offer an efficiency of about 60% on the conditions of operating temperature of 100 º C, environment temperature of 20 ºC, and radiation of 800Wm^{-2}. For the evacuated FPC collectors, they can offer work at over 50% efficiency at temperatures of 200ºC due to the high-vacuum inside. In contrast to concentrating systems, they collector can utilize diffuse irradiation and without any tracking device (TVP Solar, 2015). The thin film of a-Si cell enables easier connection with the plate and better thermal conductivity in the PV/T. A sample of a-Si cell deposited on stainless steel is shown in Figure 5.

In the practical operation the system can have three modes:

Ⅰ) The system needs to generate electricity and solar radiation is available. In this mode, valves 1, 2 and 3 are open. Pump 1 is running. The organic fluid is heated and vaporized through the collectors under high pressure. The vapor flows into the expander, exporting power in the process due to the pressure drop. The outlet vapor is cooled down in the condenser. The liquid is pressurized by pump 1

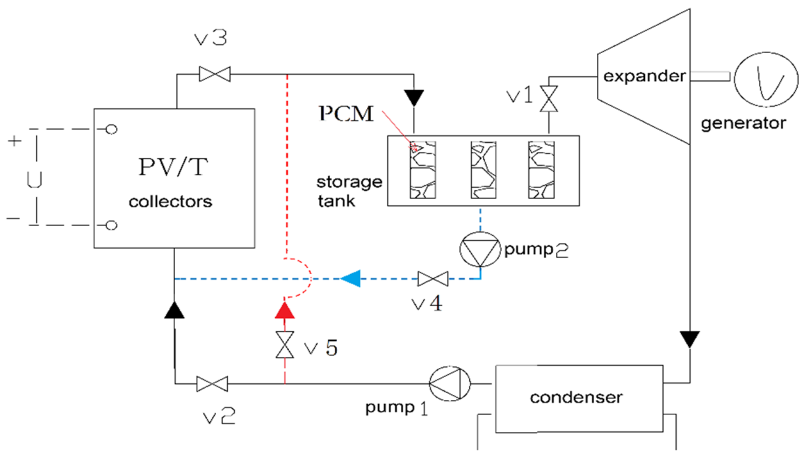

Figure 3: The scheme of the proposed HSPGS

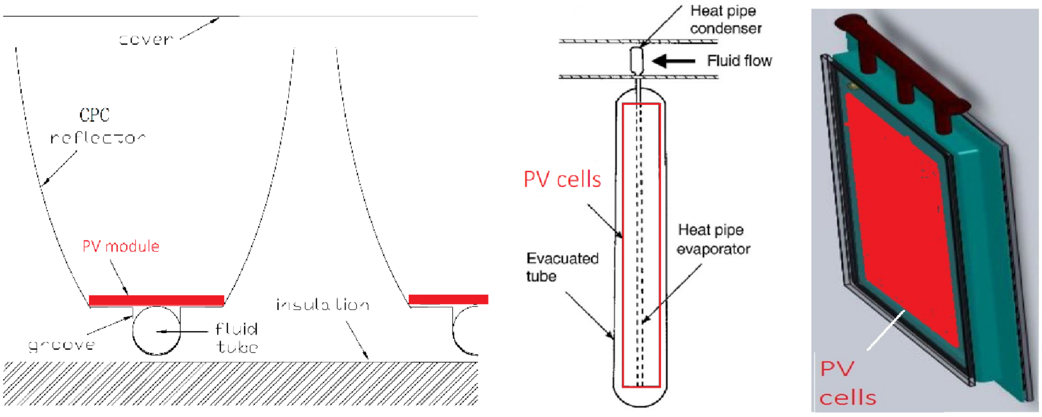

(a) CPC (b) heat pipe (c) evacuated FPC

Figure 4: Collectors suitable for medium-high temperature PV/T application

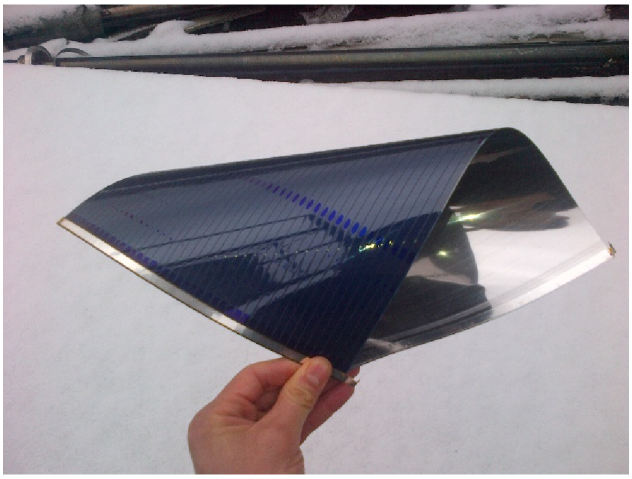

Figure 5: A sample of a-Si cell deposited on stainless steel

and is sent back to the collectors. By using a dry fluid super-heater is avoided. In case the irradiation is too strong, valve 4 can be open and pump 2 can run to prevent the working fluid from being superheated in the collectors. Aside from vapor, liquid/vapor mixture and liquid are allowed at the outlet of collectors. The liquid can drop in the fluid storage tank and won't harm the expander. Owing to this inner-type heat storage unit, the system can work smoothly without any complicated control strategy.

Ⅱ) The system does not need to generate electricity but irradiation is well. Valves 3 and 4 are open. Pump 2 is running. In this mode, solar heat is transferred to the PCM by the organic fluid. Heat storage is in process.

Ⅲ) The system needs to generate electricity but irradiation is very weak or unavailable. Valves 1 and 5 are open and pump 1 is running. Heat is released from the PCM and converted into power by the ORC. Mode Ⅰ presents the simultaneous processes of heat collection and power generation, while Mode Ⅱ or Mode Ⅲ is the independent process of heat collection or power conversion.

4. THERMODYNAMIC MODELLING

The thermal efficiency of a solar collector is generally expressed by

$$\eta_c(T) = \eta_{c,0} - \frac{A}{G}(T - T_a) - \frac{B}{G}(T - T_a)^2 \tag{1}$$

The power output of PV cell is calculated by

$$W_{PV} = G \cdot S \cdot \eta_{PV}(T) \cdot x \tag{2}$$

The heat collection efficiency of a PV/T collector can be deduced as

$$\eta_{PVT}(T) = \eta_c(T) - \eta_{PV}(T) \cdot x \tag{3}$$

If a second order of approximation of $\eta_{PV}(T)$ is assumed, then $\eta_{PV}(T) \cdot x$ can be expressed by

$$\eta_{PV}(T) \cdot x = \eta_{PV,0} + aT + bT^2 \tag{4}$$

and

$$\eta_{PVT}(T) = \eta'_{c,0} - \frac{A'}{G}(T - T_a) - \frac{B'}{G}(T - T_a)^2 \tag{5}$$

$\eta'_{c,0}$, A' , and B' are the modified coefficients of the collector.

$$\eta'_{c,0} = \eta_{c,0} - \eta_{PV,0} - aT_a - bT_a^2 \tag{6}$$

$$A' = A + (a + 2bT_a)G \tag{7}$$

$$B' = B + bG \tag{8}$$

In a solar ORC system tens or hundreds of square meters of collectors are usually required, the temperature difference between neighboring collectors is supposed to be small. The fluid in the collector is mostly at liquid-phase or binary phase. For the binary phase region, the temperature is constant and it is easy to calculate the collector efficiency. For the liquid phase region, in order to reach an outlet temperature T_o of the fluid with an inlet temperature T_i , the required collector area is obtained by

$$S_l = \int_{T_i}^{T_o} \frac{mC_p(T)}{\eta_{PVT}(T)G} dT \tag{9}$$

The heat capacity of a liquid can be expressed by a first order approximation

$$C_p(T) = C_{p,0} + \alpha(T - T_0) \tag{10}$$

With $c_1 = A'/G$, $c_2 = B'/G$, the collector area according to Equations (5), (9) and (10) is calculated by

$$S_l = \frac{m}{c_2 G(\theta_2 - \theta_1)} \left[(C_{p,a} + \alpha\theta_1) \ln \frac{(T_o - T_a - \theta_1)}{T_i - T_a - \theta_1} + (C_{p,a} + \alpha\theta_2) \ln \frac{\theta_2 - T_i + T_a}{\theta_2 - T_o + T_a} \right] \tag{11}$$

θ_1 and θ_2 are the arithmetical solutions of Equation (12)（$\theta_1 < 0,\ \ \theta_2 > 0$）.

$$\eta'_{c,o} - c_1\theta - c_2\theta^2 = 0 \tag{12}$$

$$C_{p,a} = C_{p,0} + \alpha(T_a - T_0) \tag{13}$$

The thermal efficiency of the collectors with fluid in the liquid phase is calculated by

$$\eta_{PVT,l} = \frac{m(h_{l,o} - h_{l,i})}{GS_l} \tag{14}$$

The thermal efficiency of the collectors with fluid in the binary-phase, and the overall PV/T collector efficiency are calculated by Equations (15) and (16), respectively,

$$\eta_{PVT,b} = \frac{m(h_{b,o} - h_{b,i})}{GS_b} \tag{15}$$

$$\eta_{PVT} = \frac{m(h_{b,o} - h_{l,i})}{G(S_l + S_b)} \tag{16}$$

The power generated by the cells in the liquid region of working fluid is calculated by

$$\begin{aligned} W_{PV,l} &= \int_0^{S_l} G \cdot \eta_{PV}(T) \cdot x dS \\ &= G \int_{T_i}^{T_o} \eta_{PV}(T) \cdot x \cdot \frac{mC_p(T)}{\eta_{PVT}(T)G} dT \\ &= M[N(T - T_a - \theta_1)^3 + L_1(T - T_a - \theta_1)^2 + K_1(T - T_a) + P_1 \ln(T - T_a - \theta_1)]\Big|_{T_i}^{T_o} \\ &\quad - M[N(T - T_a - \theta_2)^3 + L_2(T - T_a - \theta_2)^2 + K_2(T - T_a) + P_2 \ln(\theta_2 + T_a - T)]\Big|_{T_i}^{T_o} \end{aligned} \tag{17}$$

where

$$M = \frac{m}{c_2(\theta_2 - \theta_1)} \tag{18}$$

$$N = \frac{b\alpha}{3} \tag{19}$$

$$L_1 = 0.5[(2b\theta_1 + 2bT_a + a)\alpha + b(C_{p,a} + \alpha\theta_1)] \tag{20}$$

$$L_2 = 0.5[(2b\theta_2 + 2bT_a + a)\alpha + b(C_{p,a} + \alpha\theta_2)] \tag{21}$$

$$K_1 = \alpha[b(\theta_1 + T_a)^2 + a(\theta_1 + T_a) + \eta_{PV,0}] + (2b\theta_1 + 2bT_a + a)(C_{p,a} + \alpha\theta_1) \tag{23}$$

$$K_2 = \alpha[b(\theta_2 + T_a)^2 + a(\theta_2 + T_a) + \eta_{PV,0}] + (2b\theta_2 + 2bT_a + a)(C_{p,a} + \alpha\theta_2) \tag{24}$$

$$P_1 = [b(\theta_1 + T_a)^2 + a(\theta_1 + T_a) + \eta_{PV,0}](C_{p,a} + \alpha\theta_1) \tag{25}$$

$$P_2 = [b(\theta_2 + T_a)^2 + a(\theta_2 + T_a) + \eta_{PV,0}](C_{p,a} + \alpha\theta_2) \tag{26}$$

The power generated by the cells in the binary region of working fluid is calculated by

$$W_{PV,b} = G \cdot S_b \cdot \eta_{PV}(T_b) \cdot x \tag{27}$$

The PV efficiencies of the liquid-inside, mixture-inside and entire PV/T collectors are calculated by

$$\eta_{PV,l} = \frac{W_{PV,l}}{GS_l} \tag{28}$$

$$\eta_{PV,b} = \frac{W_{PV,b}}{GS_b} \tag{29}$$

$$\eta_{PV} = \frac{W_{PV,l} + W_{PV,b}}{G(S_l + S_b)} \tag{30}$$

The ORC efficiency is defined by the ratio of the net power output to the heat supplied,

$$\eta_{ORC} = \frac{W_t \cdot \varepsilon_g - W_p}{m(h_{b,o} - h_{l,i})} \tag{31}$$

The total efficiency of the HSPGS is

$$\eta_{HSPGS} = \eta_{PV} + \eta_{ORC} \cdot \eta_{PVT} \tag{32}$$

5. RESULTS AND DISCUSSION

To estimate the HSPGS performance, the evacuated FPC collector is exemplified. According to the test results by the international standards (EN 12975 and EN 12976), this kind of collector can have $\eta_{c,0}$ of 0.82, A of 0.399 W $m^{-2}K^{-1}$ and B of 0.0067 W $m^{-2}K^{-2}$(Test Report, 2012). In this work, modest values are chosen, and $\eta_{c,0}$, A and B are 0.75, A of 0.80 W $m^{-2}K^{-1}$ and 0.0067 W $m^{-2}K^{-2}$ respectively. The heat loss coefficients related to radiation are then closer to those of commercial evacuated-type collectors. For the cell coefficients in Equation (4), some experiment results are typified as displayed in Figure 2. The PV efficiency above 90 ºC is calculated by extending the curve. Evaporation and condensation processes are assumed to be isobaric while expansion and pressurization processes are adiabatic. The parameters in the simulation are summarized in Table 1.

Table 1: Parameters in the simulation

Parameter	Value	Parameter	Value
Ambient temperature	20 ºC	η_{PV} @ 25 ºC	6.55%
Condensation temperature	30 ºC	x	1.0
Expander efficiency	0.75	$\eta_{c,0}$	0.75
Generator efficiency	0.80	A	0.80 W $m^{-2}K^{-1}$
Pump efficiency	0.65	B	0.0067 W $m^{-2}K^{-2}$
Radiation	800 W/m^2	Working fluid	R245fa

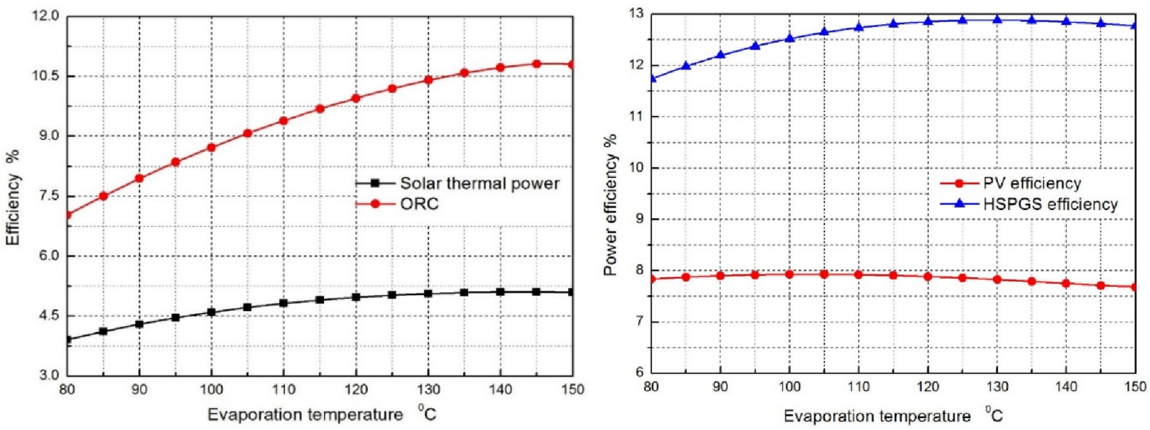

Figure 6: Efficiency variations with the ORC evaporation temperature (a) efficiencies of the ORC and solar thermal power generation, (b) efficiencies of PV cells and HSPGS

The variations of the ORC efficiency and solar thermal power efficiency ($\eta_{ORC}\cdot\eta_{PVT}$) with the evaporation temperature are shown in Figure 6(a). The ORC efficiency increases with the increment in the evaporation temperature until about 147 ºC, at which the slope of the temperature- entropy (*T-s*) curve of R245fa saturation vapor changes from positive to negative. Due to the tradeoff between the ORC efficiency and solar energy collection efficiency, the solar thermal power generation efficiency first climbs up and then falls down with increment of the evaporation temperature. It is maximum value is 5.1% with an evaporation temperature of 142 ºC.
The variations of the overall PV cells and HSPGS efficiencies with the evaporation temperature are shown in Figure 6(b). There are two effects on the PV efficiency regarding the increment in the temperature. One is the drop of the cell's open-circuit voltage (Voc), and the other is the regenerative effect promoting the cell annealing. The temperature coefficient of Voc for a-Si cell is about -0.39%/ ºC, which is generally independent on the exposure to sunlight (Ishii *et al., 2014*). The thermal annealing mainly improves the fill factor (FF). With the two competitive effects, the PV efficiency no longer decreases in a monotone way as the evaporation temperature increases. The maximum overall PV efficiency is about 7.93% at the evaporation temperature of 104 ºC. Both the efficiency and temperature at the peak point differ from those in Figure 2, which is attributed by the non-uniform temperature distribution in the PV array. The curve for the HSPGS efficiency is also like a parabola facing downward. The maximum HSPGS efficiency is 12.88% at the evaporation temperature of 130 ºC.

6. CONLUSION

In contrast to c-Si and GaAs cells, a-Si cell benefits from the thermal annealing at high temperature. The a-Si PV/T collector is an excellent match to the ORC. The efficiency of the hybrid system is much higher than that of the side by side solar ORC system (about 5.1% at 142 ºC) and PV system (about 6.55% at room temperature). Because the collectors are shared by the PV and ORC systems, the cost of the HSPGS is expected to be lower than the total cost of the side by side systems.
At present the long-term experimental study of a-Si cells at high temperature is lacked, and it is difficult to estimate the lifetime of high temperature a-Si cells. However, it is worth mentioning some points as follows: (1) Solar cells available on the market generally have a permitted operating temperature up to 85 ºC. The cell itself shall be able to operate at high temperature for years. The issue that really suffers from high temperature is the encapsulation. (2) The commercial cells are supposed to operate at normal temperature, so the encapsulation is not designed for high temperature applications. (3) High temperature PV/T systems have great potential to meet the consumers' multiple demands on cooling, spacing heating, drying and power. Research and development on this technology is being strengthened.

ACKNOWLEDGEMENT

This study was sponsored by the National Science Foundation of China (51476159, 51378483, 51206154, 51178442), Fundamental Research Funds for the Central Universities of China.

NOMENCLATURE

A	first coefficient of heat loss	($Wm^{-2}℃^{-1}$)
a	coefficient	($℃^{-1}$)
B	second coefficient of heat loss	($Wm^{-2}℃^{-2}$)
b	coefficient	($℃^{-2}$)
C	capacity	($Jkg^{-1}℃^{-1}$)
c, M, N, L, K, P	interim variables	
G	radiation	(Wm^{-2})
h	enthalpy	(J/kg)
m	mass flow rate	(kg/s)
S	area	(m^2)
T	temperature	(ºC)
W	power	(W)
x	cover ratio	
θ	arithmetical solution	
α	coefficient	($Jkg^{-1}℃^{-2}$)
ε	efficiency	
η	efficiency	

Subscript

0,1,2	reference point
a	ambient
b	binary phase
c	collector
g	generator
HSPGS	hybrid solar power generation system
i	inlet
l	liquid phase
ORC	organic Rankine cycle
o	outlet
PV	PV cell
PVT	PV/T collector
p	pressure/pump

REFERENCES

Aste, N., Leonforte, F., Del Pero, C., 2015, Design, modeling and performance monitoring of a photovoltaic–thermal (PVT) water collector. *Sol Energy*, vol. 112: p. 85–99.

Del Cueto, J., von Roedern, B., 1999, Temperature-induced changes in the performance of amorphous silicon multi-junction modules in controlled light-soaking. *Prog. Photovolt: Res. Appl.*, vol. 7, no. 2: p. 101-112.

Fanni, L., Pola, I., Burà, E., Friesen, T., Chianese, D., 2009, Investigation of annealing and degradation effects on a-Si PV modules in real operating conditions. *24th European Photovoltaic Solar Energy Conference*: p. 21-25.

Gaur, A., Tiwari, G., 2014, Performance of a-Si thin film PV modules with and without water flow: An experimental validation. *Appl Energy,* vol. 128: p.184–191.

Hanergy, thin-film solar power generation. *www.hanergy.com/en/industry/industry_310.html* 2015.05.10

Ishii, T., Otani, K., Takashima, T., Ikeda, K., 2014, Change in I–V characteristics of thin-film photovoltaic (PV) modules induced by light soaking and thermal annealing effects. *Prog. Photovolt: Res. Appl.*, vol. 22, no. 9: p. 949–957.
Ishii, T., Otani, K., Takashima, T., Kawai, S., 2011, Estimation of the maximum power temperature coefficients of PV modules at different time scales. *Sol Energy Mat Sol C,* vol. 95, no. 1: p.386–389.
Kenny, R., Chatzipanagi, A., Sample, T., 2014, Preconditioning of thin-film PV module technologies for calibration. *Prog. Photovolt: Res. Appl.*, vol. 22, no. 2: p.166 – 172.
King, D., Kratochvil, J., Boyson, W., 1997, Temperature coefficients for PV modules and arrays: measurement methods, difficulties, and results. *Photovoltaic Specialists Conference*, IEEE: p. 1183-1186.
Kosmadakis, G., Manolakos, D., Papadakis, G., 2011, Simulation and economic analysis of a CPV/thermal system coupled with an organic Rankine cycle for increased power generation. *Sol Energy*, vol. 85, no. 5: p. 308–324.
Li, J., 2015, Structural optimization of the ORC-based solar thermal power system, Chapter 2, *Structural optimization and experimental investigation of the organic Rankine cycle for solar thermal power generation*, Springer, Heidelberg: p. 41.
Li, J., Pei, G., Ji, J., 2009, A hybrid solar ORC and PV system. Chinese Patent, CN200910144276.6.
Li, J., Pei, G., Li, Y., Ji, J., 2010, Novel design and simulation of a hybrid solar electricity system with organic Rankine cycle and PV cells, *Int. J. Low-Carbon Tech.* , vol. 4, no. 5: p. 223-230.
Makrides, G., Zinsser, B., Phinikarides, A., Schubert, M., Georghiou, G., 2012, Temperature and thermal annealing effects on different photovoltaic technologies. *Renew Energ*, vol. 43: p. 407-417.
Nikolaeva‐Dimitrova, M., Kenny, R., Dunlop, E，Pravettoni, M., 2010, Seasonal variations on energy yield of a-Si, hybrid, and crystalline Si PV modules. *Prog. Photovolt: Res. Appl.*, vol. 18, no. 5: p. 311–320.
Nualboonrueng, T., Tuenpusa, P., Ueda, Y., Akisawa, A., 2012, Field experiments of PV-thermal collectors for residential application in Bangkok. *Energies*, vol. 5, no. 4: p.1229-1244.
Pathak, M., Girotra, K., Harrison, S., Pearce, J., 2012, The effect of hybrid photovoltaic thermal device operating conditions on intrinsic layer thickness optimization of hydrogenated amorphous silicon solar cells. *Sol Energy*, vol. 86, no. 9: p. 2673–2677.
Pathak, M., Pearce, J., Harrison, S., 2012, Effects on amorphous silicon photovoltaic performance from high-temperature annealing pulses in photovoltaic thermal hybrid devices. *Sol Energy Mat Sol C,* vol. 100: p. 199–203.
Rahou, M., Othman, M., Mat, S., Ibrahim, A., 2014, Performance study of a photovoltaic thermal system with an oscillatory flow design. *J Sol Energy Engineering*, vol. 136, no. 1: p.011012.
Roedern, B., del Cueto, J., 2000, Model for Staebler-Wronski degradation deduced from long-term, controlled light-soaking experiments. *MRS Proceedings,* Cambridge Univ Press: p. A10. 4.
Rozario, J., Vora, A., Debnath, S., Pathak, M., Pearce, J., 2014, The effects of dispatch strategy on electrical performance of amorphous silicon-based solar photovoltaic-thermal systems. *Renew Energ*, vol. 68: p. 459-465.
Ruther, R., Tamizh-Mani, G., del Cueto, J., Adelstein, J., Dacoregio, MM., von Roedern, B., 2005, Performance test of amorphous silicon modules in different climates - year three: higher minimum operating temperatures lead to higher performance levels. *Photovoltaic Specialists Conference*, IEEE: p.1635 – 1638.
Virtuani, A., Fanni, L., 2014, Seasonal power fluctuations of amorphous silicon thin-film solar modules: distinguishing between different contributions. *Prog. Photovolt: Res. Appl.*, vol. 22, no. 2: p. 208–217.
TVP Solar: *www.tvpsolar.com/index.php?context=news-home&liv2=news&id_news=27,* 2015.02.16.
Institut für Thermodynamik und Wärmetechnik (ITW). 2012, Test report n.11COL1028.